

# Observational determination of the time delays in gravitational lens system Q2237+0305

V. Vakulik<sup>1</sup>, R. Schild<sup>2</sup>, V. Dudinov<sup>1</sup>, S. Nuritdinov<sup>3</sup>, V. Tsvetkova<sup>4</sup>, O. Burkhonov<sup>3</sup>, and T. Akhunov<sup>3</sup>

<sup>1</sup> Institute of Astronomy of Kharkov National University, Sumskaya 35, 61022 Kharkov, Ukraine  
e-mail: vakulik@astron.kharkov.ua

<sup>2</sup> Center for Astrophysics, 60 Garden Street, Cambridge, MA 02138, USA

<sup>3</sup> Ulugh Beg Astronomical Institute of Ac.Sci. of Uzbekistan, Astronomicheskaya 33, 700052 Tashkent, Republic of Uzbekistan

<sup>4</sup> Institute of Radio Astronomy of Nat. Ac. Sci. of Ukraine, Krasnoznamenaya 4, 61002 Kharkov, Ukraine

Received 4 June 2005 / Accepted 26 October 2005

## ABSTRACT

We present new brightness monitoring observations of the 4 components of gravitationally lensed system Q2237+0305, which show detection of an intrinsic quasar brightness fluctuation at a time of subdued microlensing activity, between June 27 and October 12, 2003. These data were used to determine the time delays between the arrivals of the four images. The measured delays are  $\tau_{BA} \approx -6$ ,  $\tau_{CA} \approx 35$ , and  $\tau_{DA} \approx 2$  h, so they confirm that the long history of brightness monitoring has produced significant detection of microlensing. However the error bars associated with the delays, of order 2 days, are too large to discriminate between competing macro-imaging models. Moreover, our simulations show that for the amplitude of this intrinsic fluctuation and for photometric errors intrinsic to optical monitoring from our 1.5-m telescope or from the OGLE monitoring, a daily sampled brightness record cannot produce reliable lags for model discrimination. We use our simulations to devise a strategy for future delay determination with optical data. Nevertheless, we regard these first estimates to be significant, since they are the first direct measurements of time delays made for this system from ground-based observations in the visual wavelengths. The detected highly correlated fluctuations of the four quasar images provide an extra confirmation of the gravitational-lens nature of Q2237+0305, and give observational justification to the extensive literature which attributes the quasar's previously observed brightness fluctuations to microlensing.

**Key words.** gravitational lensing – quasars: individual: Q2237+0305 – methods: observational

## 1. Introduction

The quadruple Q2237+0305 gravitationally lensed quasar system was among the first discovered (Huchra et al. 1985; Yee 1988), and has frequently been cited as an important system in which microlensing by stars in the lens galaxy should be readily observed with events having duration of a few hundred days. However microlensing studies have ordinarily required determination of time delays to permit discrimination between intrinsic quasar fluctuations and microlensing-induced brightness fluctuations. In the case of Q2237+0305, models of the macro-imaging from the earliest times (e.g. Schneider et al. 1988; Rix et al. 1992; Wambsganss & Paczynski 1994), as well as the most recent and most popular model by Schmidt et al. (1998) all suggested that the time delays should be short, of order a few hours up to 1 day, but this prediction has never been confirmed by observations. This is because of the high optical density to microlensing for all the four quasar components; their brightness changes are unceasing and significantly uncorrelated. Till recently, the available light curves of the Q2237+0305 components did not reveal any region of correlated brightness variations, which could be attributed

to the quasar intrinsic brightness fluctuation, with one exception; Østensen et al. (1996) noted a synchronous brightening of all four components in 1994, – in the very end of their monitoring program with the Nordic Optical Telescope. It was interpreted as a possible intrinsic variation of the source, reaching 0.0006 mag per day. The authors found this to be insufficient for determining the time delays, but noted a rather high correlation between the components. A single measurement of time delay for Q2237+0305 exists so far, made by Dai et al. (2003) from the Chandra X-ray observations. They reported a 2.7 h time delay between images A and B, with image A leading.

When the first Q2237 microlensing fluctuations were announced in 1989 by Irwin et al. (1989), the Q0957 time delay had already been measured by Schild & Cholfin (1986) and confirmed by Vanderriest et al. (1989). Both authors reported evidence of microlensing in the Q0957 system (Grieger et al. 1986; Vanderriest et al. 1989), but the claim was not completely accepted because the time delay was challenged by Lehar et al. (1992) from radio data and by Press et al. (1992) from re-analysis of the optical data. However redetermination of the Q0957 time delay by Schild & Thomson (1997),

Pelt et al. (1996) and Kundic et al. (1997) firmly established the original Schild & Chofin (1986) time delay and, thus also, the first discovered microlensing event, evidently caused by a star in the lens galaxy (Schild & Smith 1991).

During the same time period, numerous events were detected in the Q2237 system and discussed in the context of microlensing even though the time delay had not been measured, but was presumed to be short (Corrigan 1991; Wambsgans et al. 1990). Thus it would be important to observationally confirm this prediction in order to validate the microlensing inferences. However because the microlensing of the individual images is seen nearly continuously, it has been difficult to date to detect an intrinsic quasar fluctuation from which the time delays could be determined. A similar conundrum has been discussed in the case of Q0957 by Colley & Schild (2003); because of the microlensing it has been difficult to determine an accurate time delay, but without an accurate time delay it has been difficult to study the microlensing.

We report below the observation of an unambiguous Q2237 intrinsic quasar fluctuation seen in all four images. In Sect. 2 we report our observations with the 1.5-m Maidanak telescope, and their reduction to form the four time series records. In Sect. 3 we determine the delays between the arrivals of the four images by two methods, and in the final sections we discuss our results in the context of intrinsic quasar fluctuations observed in other quasars, and in the context of the microlensing and macro-lensing models.

## 2. Observations and data reduction

CCD images of the Q2237+0305 gravitationally lensed quasar were taken with the Maidanak 1.5-m telescope in the framework of an international cooperative program of monitoring gravitational lenses, launched in 1997, (Dudinov et al. 2000b; Vakulik et al. 2004). An LN-cooled BroCam CCD camera with a SITe ST 005A chip was available in the f/8 focal plane, giving a scale of  $0.26''/\text{pix}$ . Magnitude measurements of the four quasar components with the corresponding uncertainties are shown in Table 1, where the Julian dates and the seeing conditions (FWHM values) are also indicated.

Because of some problems with the telescope tracking system, we used rather short exposures, which do not exceed 3 min. Therefore, to provide the highest photometric accuracy, the Q2237 images were usually taken in series, consisting of 4 to 12 frames. The frames were averaged before being subjected to photometric processing, thus ensuring the accuracy of about  $0.008^m$  for A,  $0.018^m$  for B,  $0.016^m$  for C, and  $0.020^m$  for the D component. These are the mean errors, averaged over the entire dataset, while the error values presented in Table 1 for every date were obtained from a comparison of the photometry of individual frames in the series, and may be regarded as an adequate estimate of the random error inherent in a particular quasar image component series.

The algorithm of photometric image processing is described in great details in (Vakulik et al. 2004), where the absence of seeing-dependent systematic photometric errors for images with PSF values up to  $1.4''$  is claimed. It is interesting to note as well, that the errors indicated in Table 1 reveal

no seeing dependence for PSFs up to  $1.2''$ . However, one can easily notice much larger errors for three dates, when the seeing was  $1.4''$  to  $1.5''$ .

The Q2237+0305 A, B, C, D light curves are shown in Fig. 1. To better illustrate their similarity, they are arbitrarily shifted along the magnitude axis. The upper curve is a total light curve obtained from the aperture photometry of the central part of the object within a diaphragm of  $3''$  radius, and with the subsequent subtraction of the intensity contribution from the galaxy. Polynomial fits (fifth order polynomials were used) are also shown. All light curves are well correlated, thus demonstrating extremely low microlensing activity during this time period, while the quasar revealed rather high variability,  $-0.15^m$  between the Julian dates 860 and 910, i.e. about  $0.003^m$  per day. This is almost five times more rapid brightness change as compared to the measurements by Østensen et al. (1996) in 1994. Similar synchronous brightness variations can be seen in the V light curves obtained by the OGLE group for the same time period, (<http://www.astrouw.edu.pl/~ogle/ogle3/huchra.html>), though the authors do not note similarity between the light curves of the components. A quantitative measure of similarity between the light curves can be seen from Table 2, where the corresponding correlation indices are shown for our photometry and for the OGLE data. Since the expected time delays are very short, the table justifies an attempt to undertake calculation of the time delays, which is possible thanks to subdued, though non-zero microlensing activity.

It is interesting to estimate the level of possible microlensing activity during this time period. In Fig. 2, variations of magnitudes of individual quasar components with respect to their integral light curve are shown, which are probably caused by microlensing. The figure illustrates, that the microlensing variations are rather slow and may be regarded as linear trends during the 100-day monitoring period. The mean slopes fitted to these microlensing residuals were  $-0.000136$ ,  $0.000125$ ,  $-0.000251$ , and  $0.000264$  mag per day for the A, B, C and D components, respectively. These are important quantities, which we will need in the next section to analyse uncertainties of the time delays estimates.

We tried to fit the observed brightness changes by polynomials of the 3-rd, 4-th, 5-th, and 6-th orders, and found that there is no justification to use the polynomial degree higher than four in calculations, since scatter of observational data points from the fitting curves decreases very slowly as the polynomial order grows. For example, the fourth-order polynomial gives the rms deviations for the datapoints of  $0.0148^m$ ,  $0.0228^m$ ,  $0.0161^m$ ,  $0.0206^m$ , and  $0.0098^m$  for the A, B, C and D components and the quasar, respectively, whereas with the fifth-order polynomial, the rms deviations are  $0.0147^m$ ,  $0.0227^m$ ,  $0.0159^m$ ,  $0.0204^m$ , and  $0.0098^m$ .

These values may be regarded as upper limits to the rms errors of our data, while the values  $0.008^m$ ,  $0.018^m$ ,  $0.016^m$ , and  $0.020^m$  indicated in the second paragraph of this section, should be regarded as a measure of the intrinsic convergence of the photometry for images A, B, C and D, respectively. Thus the data presented in Table 1 and shown in Fig. 1 are accurate enough to attempt calculations of time delays. Table 2 contains

**Table 1.** Photometry of Q2237+0305 A, B, C, D in the *R* band from observations with the Maidanak 1.5-m telescope in June–October 2003.

Date	JD (2 452 000+)	A	B	C	D	<i>FWHM</i> (arcsec)	Number of frames
Jun. 27	818	17.055 ± 0.003	18.549 ± 0.029	18.285 ± 0.013	18.392 ± 0.031	1.0	4
Jun. 28	819	17.071 ± 0.014	18.615 ± 0.030	18.282 ± 0.012	18.389 ± 0.014	1.0	4
Jun. 29	820	17.069 ± 0.013	18.593 ± 0.026	18.286 ± 0.015	18.450 ± 0.021	1.0	4
Jul. 01	822	17.076 ± 0.005	18.604 ± 0.023	18.272 ± 0.021	18.437 ± 0.042	0.9	7
Jul. 04	825	17.049 ± 0.008	18.533 ± 0.032	18.287 ± 0.025	18.413 ± 0.042	1.0	4
Jul. 07	828	17.053 ± 0.010	18.574 ± 0.004	18.260 ± 0.005	18.415 ± 0.008	0.9	4
Jul. 08	829	17.070 ± 0.009	18.590 ± 0.054	18.274 ± 0.032	18.424 ± 0.109	1.0	4
Jul. 10	831	17.052 ± 0.014	18.598 ± 0.035	18.310 ± 0.034	18.414 ± 0.036	1.2	6
Jul. 14	835	17.077 ± 0.005	18.605 ± 0.025	18.305 ± 0.023	18.422 ± 0.045	1.1	8
Jul. 19	840	17.086 ± 0.006	18.595 ± 0.029	18.280 ± 0.023	18.436 ± 0.021	0.9	6
Jul. 26	847	17.077 ± 0.006	18.594 ± 0.011	18.289 ± 0.020	18.439 ± 0.008	1.0	4
Jul. 28	849	17.057 ± 0.018	18.622 ± 0.015	18.280 ± 0.057	18.446 ± 0.049	1.2	4
Jul. 30	851	17.056 ± 0.003	18.585 ± 0.005	18.269 ± 0.022	18.430 ± 0.034	1.1	4
Jul. 31	852	17.069 ± 0.001	18.566 ± 0.012	18.284 ± 0.015	18.413 ± 0.012	0.9	6
Aug. 05	857	17.073 ± 0.007	18.564 ± 0.016	18.262 ± 0.012	18.416 ± 0.016	1.2	12
Aug. 06	858	17.070 ± 0.006	18.592 ± 0.009	18.246 ± 0.014	18.425 ± 0.012	0.9	4
Aug. 08	860	17.070 ± 0.004	18.570 ± 0.007	18.259 ± 0.008	18.413 ± 0.012	0.9	9
Aug. 09	861	17.072 ± 0.005	18.578 ± 0.013	18.270 ± 0.016	18.437 ± 0.014	0.8	6
Aug. 10	862	17.069 ± 0.005	18.577 ± 0.017	18.276 ± 0.015	18.435 ± 0.020	0.9	4
Aug. 11	863	17.066 ± 0.018	18.606 ± 0.046	18.236 ± 0.036	18.440 ± 0.043	1.0	5
Aug. 14	866	16.925 ± 0.009	18.454 ± 0.059	18.201 ± 0.022	18.437 ± 0.039	0.9	4
Aug. 15	867	17.019 ± 0.006	18.534 ± 0.026	18.235 ± 0.030	18.362 ± 0.019	1.1	4
Aug. 16	868	17.089 ± 0.006	18.622 ± 0.018	18.288 ± 0.012	18.427 ± 0.022	1.1	4
Aug. 21	873	17.062 ± 0.010	18.543 ± 0.015	18.242 ± 0.017	18.385 ± 0.018	0.8	4
Aug. 22	874	17.032 ± 0.004	18.555 ± 0.012	18.245 ± 0.007	18.399 ± 0.015	0.9	4
Aug. 23	875	17.048 ± 0.005	18.567 ± 0.005	18.249 ± 0.012	18.400 ± 0.019	1.0	6
Aug. 24	876	17.038 ± 0.009	18.533 ± 0.015	18.246 ± 0.006	18.413 ± 0.014	1.0	4
Aug. 25	877	17.037 ± 0.005	18.546 ± 0.012	18.237 ± 0.012	18.401 ± 0.022	1.0	4
Aug. 26	878	17.017 ± 0.006	18.525 ± 0.006	18.222 ± 0.007	18.380 ± 0.017	0.8	4
Aug. 27	879	17.039 ± 0.007	18.555 ± 0.023	18.258 ± 0.010	18.388 ± 0.011	0.8	4
Aug. 28	880	17.026 ± 0.005	18.541 ± 0.019	18.222 ± 0.004	18.394 ± 0.011	1.0	6
Sep. 01	884	17.006 ± 0.010	18.535 ± 0.022	18.193 ± 0.017	18.390 ± 0.009	1.0	4
Sep. 02	885	16.978 ± 0.032	18.583 ± 0.026	18.183 ± 0.059	18.373 ± 0.047	1.5	4
Sep. 05	888	16.981 ± 0.012	18.515 ± 0.029	18.219 ± 0.024	18.366 ± 0.036	1.1	4
Sep. 06	889	16.996 ± 0.016	18.491 ± 0.065	18.169 ± 0.057	18.282 ± 0.019	1.1	4
Sep. 12	895	16.826 ± 0.015	18.567 ± 0.227	18.089 ± 0.023	18.394 ± 0.153	1.4	4
Sep. 13	896	16.991 ± 0.003	18.533 ± 0.031	18.215 ± 0.008	18.327 ± 0.033	0.9	3
Sep. 15	898	16.924 ± 0.024	18.450 ± 0.039	18.103 ± 0.046	18.340 ± 0.051	1.5	8
Sep. 16	899	16.923 ± 0.006	18.513 ± 0.028	18.154 ± 0.033	18.395 ± 0.048	1.2	4
Sep. 17	900	16.975 ± 0.003	18.471 ± 0.007	18.201 ± 0.004	18.310 ± 0.014	0.9	12
Sep. 18	901	16.953 ± 0.008	18.499 ± 0.010	18.157 ± 0.011	18.358 ± 0.014	0.9	8
Sep. 19	902	16.946 ± 0.004	18.473 ± 0.010	18.142 ± 0.007	18.319 ± 0.012	1.1	8
Sep. 20	903	16.937 ± 0.003	18.466 ± 0.004	18.151 ± 0.012	18.305 ± 0.013	0.8	4
Sep. 21	904	16.923 ± 0.005	18.465 ± 0.010	18.123 ± 0.016	18.308 ± 0.011	1.2	8
Sep. 24	907	16.924 ± 0.006	18.487 ± 0.011	18.144 ± 0.003	18.325 ± 0.011	1.0	6
Sep. 25	908	16.933 ± 0.004	18.470 ± 0.013	18.135 ± 0.010	18.331 ± 0.010	0.9	8
Sep. 27	910	16.928 ± 0.008	18.503 ± 0.019	18.139 ± 0.025	18.311 ± 0.016	1.2	6
Sep. 29	912	16.917 ± 0.007	18.440 ± 0.010	18.115 ± 0.010	18.329 ± 0.010	1.2	7
Sep. 30	913	16.927 ± 0.002	18.469 ± 0.003	18.133 ± 0.007	18.313 ± 0.004	0.8	8
Oct. 01	914	16.932 ± 0.005	18.470 ± 0.011	18.138 ± 0.015	18.323 ± 0.006	0.9	4
Oct. 02	915	16.929 ± 0.003	18.476 ± 0.008	18.126 ± 0.006	18.329 ± 0.004	0.8	8
Oct. 11	924	16.938 ± 0.003	18.479 ± 0.011	18.137 ± 0.009	18.315 ± 0.009	0.9	8
Oct. 12	925	16.920 ± 0.005	18.433 ± 0.009	18.117 ± 0.007	18.287 ± 0.012	1.0	4

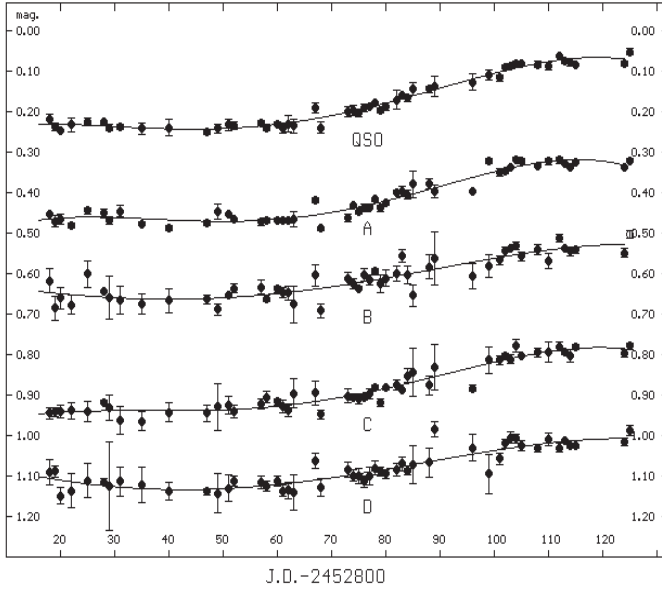


**Fig. 1.** Synchronous variations of brightnesses of the A-D images observed in Q2237+0305 between June 27 and October 12, 2003 with the Maidanak 1.5-m telescope. *R* magnitudes shifted arbitrarily along the vertical axis are shown. The upper curve is an integral light curve of the four quasar images (see the text for more details).

**Table 2.** Correlation indices between the light curves of the Q2237 components calculated for our data, and for the OGLE photometry. Quantities in the last line and column of the first table, both marked as QSO, are correlation indices between a particular light curve and the integral light curve of the quasar.

<i>Our data</i>					
Component	A	B	C	D	QSO
A	1	0.899	0.960	0.874	0.978
B	0.898	1	0.888	0.887	0.924
C	0.960	0.888	1	0.874	0.968
D	0.874	0.887	0.874	1	0.922
QSO	0.978	0.924	0.968	0.922	1
<i>OGLE data</i>					
Component	A	B	C	D	
A	1	0.945	0.953	0.798	
B	0.945	1	0.914	0.754	
C	0.953	0.914	1	0.726	
D	0.798	0.754	0.726	1	

an additional argument in favour of such an attempt, – the light curves of all the four quasar images are well correlated.

Nevertheless, to be sure that such low-amplitude brightness features are really capable of providing reliable estimates of time delays, to investigate the effects of photometry errors and residual microlensing effects, and to obtain consistent estimates of the time delay uncertainties, numerical simulations involving over 2000 statistical trials were undertaken. The simulation results will be briefly described at the end of the next section, after the methods used to determine time delays are presented.

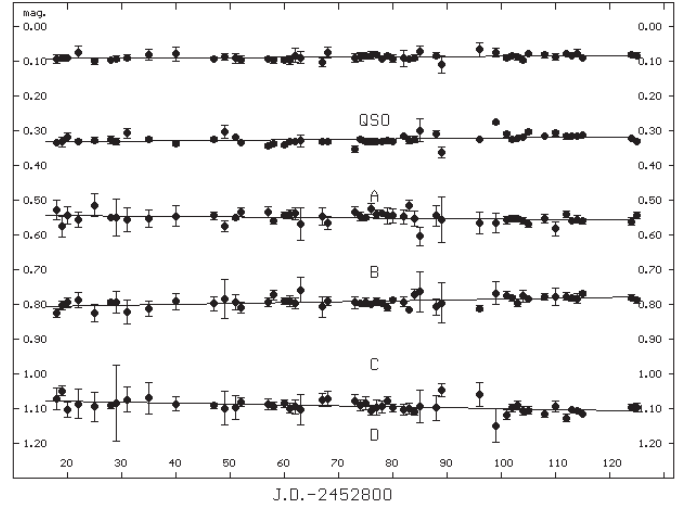


**Fig. 2.** Residual variations of brightnesses of the A-D images taken from the light curves of June 27–October 12, 2003 (Fig. 1) by subtracting the integral quasar light curve. These residuals may be treated as a result of microlensing.

### 3. Time delay estimation

The detection of correlated variations of brightnesses of the Q2237 components is important in itself, since it is the most convincing evidence of the gravitational lensing nature of the system. The deeper value of these observations is in the possibility to estimate the time delays between the brightness fluctuations seen in different lensed quasar images.

Estimation of time delays from the actual light curves, with their inevitable uneven sampling and poor statistics, is a rather difficult problem. Many approaches to solve it have been elaborated, as summarized recently by Gil-Merino et al. (2002). All of these algorithms are devised for the situation when the characteristic timescale of the quasar brightness variations and sampling time intervals of observations are much less than the expected time delays. The existing macrolensing models for this system predict time delays which do not exceed a day. Therefore, we have a somewhat atypical situation, – we are trying to estimate the time delays from brightness variations with the characteristic timescale much larger than the expected value of the time delay. Moreover, we used photometry data averaged within a night, and thus the sampling time interval exceeds the expected values of time delays too.

Taking all this into account, we used the following approach. We admit that the quasar brightness variations are rather slow and can be represented accurately enough by a fourth or fifth order polynomial. Then, representing brightness variations of a component, e.g. A, with a smooth curve  $f_A(t)$ , we may calculate a normalized cross-correlation function (NCCF) of this smooth curve with the actual light curve of another component, say, B, represented by discrete data points:

$$k(\tau) = \frac{\frac{1}{n} \sum_{i=1}^n [f_A(t_i + \tau) - \bar{f}_A(\tau)][m_B(t_i) - \bar{m}_B]}{(\sigma_f^2 \sigma_m^2)^{1/2}}, \quad (1)$$

where  $m_B(t_i)$  are discrete brightness samples at the time moments  $t_i$ ,  $f_A(t_i + \tau)$  are corresponding values of the

approximating polynomial at the time moments  $t_i + \tau$ ,  $\bar{f}_A$  and  $\bar{m}_B$  are corresponding average values, and  $\tau$  is the time shift. The average values  $\bar{f}(\tau)$ ,  $\bar{m}$  and variances  $\sigma_f^2, \sigma_m^2$  are calculated according to formulas:

$$\bar{f}(\tau) = \frac{1}{n} \sum_{i=1}^n f(t_i + \tau), \quad \bar{m} = \frac{1}{n} \sum_{i=1}^n m(t_i); \quad (2)$$

$$\sigma_f^2(\tau) = \sum_{i=1}^n \frac{[f(t_i + \tau) - \bar{f}(\tau)]^2}{n-1}, \quad \sigma_m^2 = \sum_{i=1}^n \frac{[m(t_i) - \bar{m}]^2}{n-1}. \quad (3)$$

With such an approach, we expect to find cross-correlation peaks at the cosmological lags. We adopted this procedure because it is less sensitive to bias by any false peaks for 0 lag that can result from the kinds of correlated brightness fluctuations at 0 lag when working with discrete data available from optical monitoring. These correlated photometry errors are expected from the inevitable residual sensitivity of the photometry to seeing effects, that is often observed, (e.g. Vakulik et al. 2004). The effect of such “zero lag” is also discussed in Colley et al. (2003) and interpreted as a “frame-to-frame correlation error in the photometry”.

The NCCF, calculated in this way, is a smooth function, with one maximum, which changes very slowly, and does not have other local extrema at least within  $-10 < \tau < 10$  days. It allows us to unambiguously interpret the location of the maximum of this function as an optimal value of the lag, which we accept as the time delay between the brightness variations of two components. In this way we can estimate the time delays for the light curves of all the components with respect to the fitting curve of the A component.

Similar calculations can be made with respect to the fitting curves of other components, and thus a complete set of the time delay estimates will be obtained. Such estimates cannot be regarded as independent ones however, since they are affected with the same random errors of light curves of the “template” components, while their differences are caused by the difference between the approximating curves used.

We also propose a more general approach, consisting in a joint fitting of all the four light curves by a single polynomial, with a normalizing factor, magnitude shift, and time shift of each particular light curve being treated as unknown parameters and found from a condition:

$$\sum_j \sum_i [k_j f(\mathbf{a}, t_i, \tau_j) + a_{0,j} - m_j(t_i)]^2 = \min, \quad (4)$$

$$f(\mathbf{a}, t_i, \tau_j) = \sum_{n=1}^N a_n (t_i + \tau_j)^n. \quad (5)$$

Here,  $i$  is a number of a data point in the light curve of the  $j$ th component,  $k_j$  is a normalizing factor for the  $j$ th light curve, and  $\tau_j$  is the unknown time delay for the  $j$ th component. The function  $f(\mathbf{a}, t_i, \tau_j)$  is an  $N$ th order polynomial without the zeroth order term which is represented for each component separately as the magnitude shift  $a_{0,j}$ .

These two approaches, – which we marked as NCCF and JFM (joint fitting method), – have been applied to the photometry data of June–October 2003, presented in Table 5 and

**Table 3.** Estimates of time delays for Q2237+0305 system with respect to the A image, (hours), taken with different approaches from the Maidanak data, and from those of the OGLE group. The estimates averaged over NCCF and JFM for both Maidanak and OGLE data are also shown, (weighted average values). The JFM<sub>1</sub> and JFM<sub>2</sub> columns are shown just to illustrate the attempt to equalize the amplitudes of the light curves, and they were not used to calculate the average time delays.

<i>Maidanak data</i>				
Im. pairs	NCCF	JFM	JFM <sub>1</sub>	JFM <sub>2</sub>
BA	$-13.2 \pm 59$	$-16.1 \pm 62$	33.1	-36.2
CA	$-31.9 \pm 42$	$-37.2 \pm 42$	36.9	-10.6
DA	$6.0 \pm 60$	$5.0 \pm 63$	9.1	-40.1
<i>OGLE data</i>				
BA	$1.6 \pm 52$	$5.0 \pm 57$	–	7.2
CA	$105.8 \pm 40$	$105.1 \pm 43$	–	117.8
DA	$-5.9 \pm 152$	$-3.6 \pm 156$	–	17.8
<i>Average</i>				
BA	$-6 \pm 41$			
CA	35			
DA	$2 \pm 44$			

shown in Fig. 1. The estimates of time delays of the B, C and D images with respect to image A are presented in Table 3. Column 2 contains the estimates, taken with the NCCF method. They are the results of averaging the time delay estimates calculated with respect to the fitting curves of all the components separately. In Col. 3, results of applying the JF method are shown. A comparison of these two columns illustrates the validity of both methods, – they produce almost the same time delay values.

If, in addition to the quasar intrinsic brightness changes, microlensing brightness variations took place during our monitoring time period, this might cause certain bias in the time delays estimates, and difference in the amplitudes  $k_j$  determined from (4). With the assumption that there were no strong microlensing events during our monitoring, possible minor effects of microlensing at the time interval of 100 days can be approximately represented by linear trends (see Fig. 2). To check a suggestion that the observed amplitude difference results from microlensing of the components, we changed Eq. (4), having introduced, in addition to the constant terms  $a_{0,j}$ , linear terms of the polynomial as well,  $a_{1,j}$ , for each component separately:

$$\sum_j \sum_i [k_j f(\mathbf{a}, t_i, \tau_j) + a_{0,j} + a_{1,j}(t_i + \tau_j) - m_j(t_i)]^2 = \min. \quad (6)$$

With this modification of the JFM, which we called JFM<sub>1</sub>, the averaged linear terms of the components would represent a linear term of the quasar brightness variation, while their difference might be interpreted as the effects of weak microlensings of individual components. If this were a case, such a procedure would equalize the amplitudes of the components, but this does not happen. The amplitudes can also be equalized forcedly by assuming  $k_j \equiv 1$  for all the  $j$ -s in condition (6),

(JFM<sub>2</sub> modification of the JFM). After such a procedure, however, residuals in Eq. (4) became much larger than for the JFM and JFM<sub>1</sub>, – the light curves just stopped being similar, – and this finally rejects a possibility for the amplitudes to be equalized by introducing microlensing trends.

Therefore, our assumption that the quasar brightness variation is observed in different components with different amplitudes because of microlensings does not get a solid confirmation. It should be noted also, that the time delays calculated with the JFM<sub>1</sub> are less reliable as compared to those obtained with the JFM, since the JFM<sub>1</sub> deals with a larger number of unknown parameters. Taking all this into account, we placed the results of applying the JFM<sub>1</sub> and JFM<sub>2</sub> in Table 3 (Cols. 4 and 5), but did not use them in calculations of the average time delays (the bottom of Table 3). Possible reasons for the observed difference in light curves amplitudes will be discussed in Sect. 5.

A 4th order polynomial was used for fitting in all cases. Further increasing of the polynomial order does not improve the accuracy of fitting, and further simulation shows that the random error of time delay determination increases slightly as the polynomial degree grows.

To determine reliability of estimates, and to analyse the effects of random photometric errors, numerical simulations were undertaken. The eighth-order polynomial fit to the image A light curve was adopted as an intrinsic quasar brightness curve template. Thus we admitted, that the actual brightness variation of the quasar might be more complicated as compared to the 4th order polynomial fit used for time delay estimations. Individual light curves of the components were then constructed by adding to the template curve, at the time moments corresponding to those of observations, the random noise quantities with the rms values of 0.015<sup>m</sup>, 0.023<sup>m</sup>, 0.016<sup>m</sup>, and 0.021<sup>m</sup> inherent in photometry for images A, B, C and D, respectively. A zero time lag was adopted for all the images, and 2000 random samples for each quaternary of images were formed for the simulation. The algorithms described in the previous section were applied to the random samples to calculate the average time delays with respect to image A, and their rms deviations. The estimates of time delays from these simulated samples did not reveal any noticeable biases, and the rms errors turned out to be about 62, 42 and 63 h for B, C and D, respectively.

We have also considered the possibility that a small amount of systematic microlensing could influence these time delay determinations. We have simulated the effects of such small systematic microlensing as a sustained brightness increase (decrease) during 100 days of our monitoring. To do this, the actual light curves were distorted by linear trends, and the resulting time delay biases were estimated. For our low amplitude trends, the biases of the time delay estimates were found to depend almost linearly on the value of trend, with 1 day for the daily rate of 0.0005<sup>m</sup>. In Sect. 2, (see also Fig. 2) the maximal possible value of a microlensing trend has been estimated to be about 0.00025<sup>m</sup> per day. Therefore, the maximum possible time delay bias caused by uncompensated microlensing events does not exceed 12 h.

We also tried to calculate the time delays using the OGLE data, (<http://www.astrouw.edu.pl/~ogle/ogle3/huchra.html>). The results of applying the NCCF and JF methods are shown in Table 3, (Cols. 2 and 3), as well as the attempts to equalize the amplitudes of the OGLE light curves, (JFM<sub>2</sub> column). The results show, that the high accuracy inherent in the OGLE photometry, does not seem to improve the results. The error estimates resulting from our simulations as above, are still very large, and the time delays differ from the values predicted from available macro-imaging models.

The results of averaging the estimates taken with the NCCF and JFM for both the Madaanak and OGLE light curves are also shown in Table 3, where the weighted average values are given. The time delays determined from the Madaanak and OGLE data are seen to be well within the indicated error bars for the AB and AD pairs, while for the AC pair, the difference between the estimates obtained from the two data sets is much larger than the error bar calculated from the simulations. In this case, it would not be reasonable to indicate any error bar, and therefore no table entry is given for the AC pair error.

In the following sections, we analyse these results and discuss the pitfalls and prospects of observational measurement of time delays for the Q2237+0305 system, from daily sampled optical wavelength data.

#### 4. Time delay predictions for Q2237 from macro-imaging models

The first predictions of time delays for the Q2237+0305 system appeared soon after its identification as a quasar quadruply imaged by the gravitational field of a foreground galaxy, (Schneider et al. 1988; Kent & Falco 1988). Schneider et al. (1988) treated the lensing galaxy projected mass distribution as proportional to the observed light distribution and found that “a constant mass-to-light ratio, elliptical, de Vaucoulers bulge reproduces the observed configuration remarkably well.” The model was improved in 1992 with the use of a more accurate galaxy light distribution using the Hubble Space telescope data (Rix et al. 1992). Kent & Falco (1988) used another approach and considered elliptical mass distributions with a de Vaucoulers and a King profile mass distribution. Another way to account for the mass distribution ellipticity was proposed, e.g., by Kochanek (1991) and Wambsganss & Paczynski (1994). They used a shear,  $\gamma$ , while the mass distribution in the lens was adopted to be spherically symmetric, – a singular isothermal sphere and a point mass plus different types of the shear, (Kochanek 1991), and a singular power-law sphere with an external shear (Wambsganss & Paczynski 1994). A massive disk with a central nucleus as a point mass, isothermal sphere and Plummer’s sphere were also considered as models for the Q2237 lensing galaxy, (Minakov & Shalyapin 1991). An attempt to account for the galaxy bar should be mentioned also, (Schmidt et al. 1998). They used two-dimensional Ferrers profiles for the mass distribution in the bar, and a power-law elliptical mass distribution for the bulge, with the bar representing a small perturbation of the deflecting field of the bulge and constituting about 5% of the bulge mass in the region inside the quasar images.

**Table 4.** Model predictions for the time delays  $\tau_{BA}$ ,  $\tau_{CA}$ , and  $\tau_{DA}$  for Q2237+0305 system, (hours).

Reference	Lens model	$\tau_{BA}$	$\tau_{CA}$	$\tau_{DA}$
Schneider, et al. (1988)	Constant mass-to-light ratio	-2.4	-29.5	-26.6
Rix et al. (1992)	Model 1	2.1	11	7.1
	Model 2	1.5	10.1	6.1
	Model 2a	-1.7	9.8	3.7
Wambsganss & Paczynski (1994)	Point lens	-2.97	17.41	4.87
	Isothermal sphere	-1.51	8.91	2.46
	Best fit	-0.44	2.54	0.7
Schmidt, et al. (1996)	Bar accounted	-2.0	16.2	4.9

Predictions of the time delays for the Q2237 images that we could find in the works cited above, are collected into Table 4, with the proper referencing and brief comments concerning each particular model used. Here, Models 1 and 2 by Rix et al. (1992) mean, respectively,  $R^{1/4}$  profile,  $R^{1/4}$  plus unresolved nucleus, and Model 2a means Model 2 with only image positions matched. The predicted values of time delays are seen to be obviously model dependent. The values of the expected time delays calculated by Wambsganss & Paczynski (1994) exhibit a tendency to decrease as the index of power  $\beta$  in their power-law mass profile grows – from  $\beta = 0$  for a “point lens”, through  $\beta = 1$  for an isothermal sphere, and up to  $\beta = 1.71$ , (“best fit model”). The B component is always leading, in contrast to the model by Rix et al. (1992). A rather good agreement of their point lens model predictions with those by Schmidt et al. (1998) should be noted, where the effect of the galaxy bar was taken into account.

In light of the errors and simulations presented in Sect. 3, we can make no conclusions about the comparison of models with our lag calculations from monitoring data.

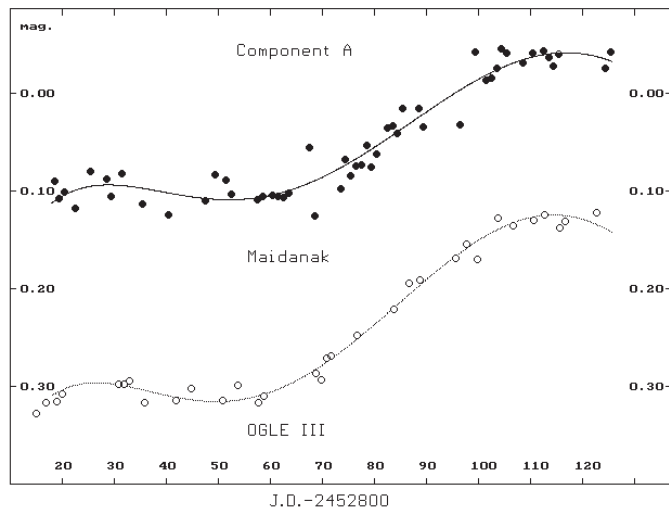
## 5. Quasar intrinsic brightness fluctuation amplitude

In analysing our calculations, one more thing should be noted and discussed. It has been shown in Sect. 2 (see Table 2), that the light curves of all the components are highly correlated, both in the  $R$  filter (our observations), and in the  $V$  band (OGLE data). It should be noted however that the  $R$  light curves built from the same Maidanak data by the Moscow group, (Koptelova et al. 2005) differ from our light curves, with the cross correlation indices being much lower than those shown in Table 2, and ranging from 0.2 to 0.7.

If the light curves observed during the time period from June 27 to October 12, 2003, represent a quasar intrinsic brightness change, then its amplitude seen in different lensed images is believed to be the same. As seen from Table 5, where the amplitudes of our  $R$  light curves and those of the OGLE group in the  $V$  band are presented in the units of “our” A component amplitude, this is not the case. The amplitudes of the A and

**Table 5.** Relative amplitudes of  $R$  light curves, (our data), and light curves in  $V$  (OGLE data) calculated for the time period June 27–October 12, 2003.

Image	$R$	$V$
A	1.000	1.263
B	0.809	0.796
C	1.004	0.854
D	0.751	0.370

**Fig. 3.**  $R$  light curve of image A from observations on Maidanak in June 27–October 12, 2003, (our photometry), – upper curve, solid circles, – and  $V$  light curve of image A built from the OGLE data, – bottom curve.

C light curves are noticeably larger than that of D both from our data and from the OGLE group data. Inconsistencies between our measurements and the OGLE data can also be seen from this table. To better demonstrate what kind of inconsistencies between the Maidanak and OGLE data take place, – and, at the same time, how similarly they look, – we plotted our  $R$  and the OGLE  $V$  light curves of image A in the same picture, (Fig. 3).

A possible explanation of these complex differences in fluctuation amplitude may be the following. We adopt the picture that all four image components may be microlensed but far enough from a caustic in the microlensing pattern that almost no change in relative brightnesses of the 4 images is seen during our monitoring period. It is also possible that the microlensing caustic pattern in the four images is moving approximately parallel to the local caustic structure. It is known that microlensing can cause an image to become bluer as the caustics cross the quasar structure and magnify most strongly the bluest innermost region (Wambsganss & Paczynski 1991; Vakulik et al. 2004). Presumably at the 2003 time of these observations, image A was brightest (and image B was faintest) because of microlensing image magnification (demagnification). Such magnification can alter the color of the images as noted previously, and depending upon the details of which part of the image are most strongly microlensed, and which part of

the quasar became brighter in the course of the quasar intrinsic brightness fluctuation, color microlensing effects of several kinds might be expected. These topics have not been explored with extensive simulations to date, because there is as yet no standard quasar model. We also note the possibility that the unequal amplitudes might result in part from complex structure in either the quasar image (Schild & Vakulik 2003), or in the lens galaxy. In the latter case, a subtle unresolved lens galaxy brightness feature might cause the erroneous estimation of an individual image brightness; however we would expect this to have been noticed in other Q2237 data analysis.

We also note a possible artifact from systematic errors in image processing that have been discussed already in a number of publications, (Alcalde et al. 2002; Burud et al. 1998; Vakulik et al. 2004). Because of closeness of quasar images to the galaxy nucleus and to each other, errors of processing due to incorrect subtraction of foreground galaxy light or due to incorrect subtraction of light from the other images are possible, and different for different photometry methods.

## 6. Strategy to detect time delays

The interesting X-ray observation of possible 2.7 h time delay between the A and B images (Dai et al. 2003) raises the question of limits of our ability to measure with precision the lags for all four images from optical data. In spite of years of Q2237 brightness monitoring, little is yet known about the quasar's intrinsic brightness fluctuations on long or short time scales.

On short time scales, Burud et al. (1998) and Cumming et al. (1995) monitored Q2237 intensively for three nights with the NOT and with the CFHT. And nightly monitoring by Vakulik et al. (2004) for 46 nights in 2000 with the R filter precludes fluctuations of more than 1%.

We can also recall what is known about rapid fluctuations in other quasars. Colley & Schild (2003) present convincing evidence for Q0957 nightly brightness fluctuations at the level of 0.01 mag (their Fig. 1). Gopal-Krishna et al. (2003) report detection of intranight variations of brightness of about 0.01–0.02 mag in their sample of radio-quiet quasars. At the same time, in a survey of 23 high-luminosity ( $-27 < M_V < -30$ ) radio-quiet quasars by Rabbette et al. (1998), “no evidence for short-term variability greater than about 0.1 mag was detected in any of the 23 sources”.

Long-term variability of quasars is rather well documented with the use of huge amounts of observational data, – e.g., results of statistical processing of a sample containing over 40 000 quasars as reported by de Vries et al. (2005). Structure function analysis of this sample produced estimates of short-term variability consistent with the above, and also produced some important statistical characteristics of the variability of quasars, with the following ones relevant here: 1) the increase of variability with increasing time lags is monotonic and constant up to time-scales of  $\sim 40$  years; 2) variability increases toward the blue part of the spectrum; and 3) high-luminosity quasars vary less than low-luminosity quasars.

Using this information, and based upon the results of this paper, we propose the following strategy for future attempts to

observationally determine the time delays for the Q2237+0305 gravitationally lensed quasar:

- since variability of quasars tends to increase towards the shorter wavelength, that is found for a sample of quasars by de Vries et al. (2005), and also detected for the Q2237 system, (Vakulik et al. 2004), observations should be shifted as much as possible to shorter optical wavelengths;
- monitoring should be in sets with durations of several weeks and sampling intervals of hours;
- observations should be made under the image quality of 0.6–0.7'' and better, and with the photometry accuracy of 0.005<sup>m</sup> and higher.

## 7. Conclusions

1. Variations of brightness of the four quasar images of Q2237+0305, observed during almost 100 days in June–October 2003, are due mainly to the quasar intrinsic brightness change. Microlensing activity was substantially subdued during this time period and did not exceed 0.00025 mag per day.
2. The estimates of time delays obtained with the two methods proposed, are consistent with each other, but differ from those predicted by the existing macro-imaging models. The resulting error bars neither confirm nor rule out any of the competing models.
3. The ultimate limits of time delays estimation from the available observations were tested in simulations and have shown that, with the particular type of the quasar variability, particular photometric errors and contribution from microlensing activity, one should not expect better results and higher accuracy.
4. The measured time delays between the 4 quasar images are much shorter than the time scales of observed optical microlensing brightness changes. Therefore the long history of analysing brightness changes in the Q2237 literature is based upon a correct belief that the observed fluctuations are due mainly to microlensing events. However, the detected brightness change of the quasar,  $-0.15^m$  between the Julian dates 860 and 910, i.e. about 0.003<sup>m</sup> per day, – demonstrates that the quasar intrinsic variability may noticeably contribute to the observed light curves of the components, and thus it should be taken into account when analysing and interpreting statistics of microlensing in the system.

*Acknowledgements.* The work has been substantially supported by the STCU grants NN43 and U127, and by the joint Ukrainian-Uzbek Program “Development of observational base for optical astronomy on Maidanak Mountain”. We also gratefully acknowledge the use of data obtained by the German-Uzbek collaboration between Potsdam/Heidelberg University (Robert Schmidt, Joachim Wambsganss), and Astrophysical Institute Potsdam (Stefan Gottlöber, Lutz Wisotzki), which is supported by the Deutsche Forschungsgemeinschaft under grant 436 USB 113/5/0-1.

**References**

- Alard, C., & Lupton, R. H. 1998, *ApJ*, 503, 325
- Alcalde, D., Mediavilla, E., Moreau, O., et al. 2002, *ApJ*, 572, 729A
- Burud, I., Stabell, R., Magain, P., et al. 1998, *A&A*, 339, 701
- Colley, W. N., & Schild, R. 2003, *ApJ*, 594, 97
- Colley, W. N., Schild, R. E., Abajas, C., et al. 2003, *ApJ*, 587, 71
- Corrigan, R. T., Irwin, M. J., Arnaud, J., et al. 1991, *AJ*, 102, 34
- Cumming, C. M., & De Robertis, M. M. 1995, *PASP*, 107, 469
- Dai, X., Chartas, G., Agol, E., et al. 2003, *ApJ*, 589, Iss.1, 100
- de Vries, W. H., Becker, R. H., White, R. L., & Loomis, C. 2005, *AJ*, 129, Iss. 2, 615
- Dudinov, V., Bliokh, P., Paczynski, P., et al. 2000, *Kin. & Phys. Cel. Bodies*, Suppl. No 3, 170
- Irwin, M. J., Webster, R. L., Hewett, P. C., et al. 1989, *AJ*, 98, 1989
- Gil-Merino, R., Wisotzki, L., & Wambsganss, J. 2002, *A&A*, 381, 428
- Gopal-Krishna, Stalin, C. S., Sagar, R., & Wiita, P. J. 2003, *ApJ*, 586, Iss. 1, L25
- Grieger, B., Kayser, R., & Refsdal, S. 1986, *Nature*, 324, 126
- Huchra, J., et al. 1985, *AJ*, 90, 69
- Kent, S. M., & Falco, E. E. 1988, *AJ*, 96, 1570
- Kochanek, C. S. 1991, *ApJ*, 373, 354
- Koptelova, E. A., Shimanovskaya, E. V., Artamonov, B. P., et al. 2005, *MNRAS*, 356, Iss.1, 323
- Kundic, T., Turner, E. L., Colley, W. N., et al. 1997, *ApJ*, 482, 75
- Lehar, J., Hewitt, J. N., Roberts, D. H., & Burke, B. F. 1992, *ApJ*, 384, 453
- Minakov, A. A., & Shalyapin, V. N. 1991, *Sov. Astron. Letters*, 17, 140
- Østensen, R., Refsdal, S., Stabell, R., et al. 1996, *A&A*, 309, 59
- Pelt, J., Kayser, R., Refsdal, S., & Schramm, T. 1996, *A&A*, 305, 97
- Press, W. H., Rybicki, G. B., & Hewitt, J. N. 1992, *ApJ*, 385, 404
- Rabbette, M., Mc Breen, B., Smith, N., & Steel, S. 1998, *A&AS*, 129, 445
- Rix, H.-W., Schneider, D. P., & Bachcall, J. N. 1992, *AJ*, 104, 959
- Schild, R. E., & Cholfin, B. 1986, *ApJ*, 300, 209
- Schild, R., & Smith, R. C. 1991, *AJ*, 101, 813
- Schild, R. E., & Thomson, D. J. 1997, *AJ*, 113, 130
- Schild, R., & Vakulik, V. 2003, *AJ*, 126, 689
- Schmidt, R., Webster, R. L., & Lewis, G. F. 1998, *MNRAS*, 295, 488
- Schneider, D. P., Turner, E. L., Gunn, J. E., et al. 1988, *AJ*, 95, 1619
- Vakulik, V. G., Schild, R. E., Dudinov, V. N., et al. 2004, *A&A*, 420, 447
- Vanderriest, C., Schneider, J., Herpe, G., et al. 1989, *A&A*, 215, 1
- Wambsganss, J., Paczynski, B., & Schneider, P. 1990, *ApJ*, 358, L33
- Wambsganss, J., & Paczynski, B. 1991, *AJ*, 102, 864
- Wambsganss, J., & Paczynski, B. 1994, *AJ*, 108, 1156
- Yee, H. K. C. 1988, *AJ*, 95, 1331